

## SUPPLEMENTAL INFORMATION

### Supplemental Figure Legends

**Figure S1. Representative flow cytometry and effect of ATG7 on HepG2 cells. Related to Figure 1.** (A) Flow cytometry analysis of CD133<sup>+</sup> cells of HepG2 with various treatments or with stable expression of the control shRNA or the Atg5 shRNA. (B) Flow cytometry analysis of CD133<sup>+</sup>CD49f<sup>+</sup> cells in liver tumors of control mice and ATG5-knockout mice that had been treated with DEN. (C)-(E) HepG2 cells without treatment (None) or with the stable expression of control shRNA (sh-Ctrl) or ATG7 shRNA (sh-Atg7) were subjected to immunoblot analysis (C), flow cytometry analysis of CD133<sup>+</sup> cells (D) or sphere-formation assay (E).

**Figure S2. Analysis of the effect of PFT $\alpha$  on p53. Related to Figure 2.** (A) Analysis of the effect of PFT $\alpha$  on p53 and its subcellular localization. Cytoplasmic and nuclear lysates of HepG2 cells that had been treated with PFT $\alpha$  or DMSO for one day were lysed and separated into cytoplasmic and nuclear fractions for immunoblot analysis. (B) Analysis on the effect of PFT $\alpha$  on cell viability. The viability of HepG2 cells treated with DMSO or PFT $\alpha$  were analyzed by the MTT assay.

**Figure S3. Effects of ATG5 on p53. Related to Figure 3.** (A) Immunoblot analysis of liver tumors of control mice and ATG5-KO mice that had been treated with DEN. (B) The level of p53 mRNA in HepG2 cells with various treatments for 24 hours or with stable ATG5 knockdown were quantified by real-time RT-PCR. No significant difference of p53 mRNA levels was observed.

**Figure S4. Analysis of the effect of p53 on the *NANOG* promoter. Related to Figure 4.** (A) The nucleotide sequence of the Nanog promoter that contains the putative p53-response element (highlighted in yellow color) and the OCT4-SOX2 binding site (highlighted in blue color). The consensus sequence of the p53 binding site is shown below the *NANOG* promoter sequence. R, A and G; W, T and A; and Y, T and C. (B) The supershift assay using the anti-p53 antibody that recognized phosphoserine-392. The supershift assay was conducted as shown in Figure 4D, with the exception that an increasing amount of the antibody was used for the supershift assay. (C) Effects of various p53 constructs on the *NANOG* promoter in Huh7 cells. Huh7 cells were co-transfected with the Nanog-luc2 reporter and the control vector or the expression plasmid for p53(WT), p53(S392A) or p53(S392D). The reporter pSV-RL, which

expressed renilla luciferase, was included in the transfection to monitor the transfection efficiency. The luciferase activity expressed from the parental vector pGL3-basic was arbitrarily defined as 1. The results represent the mean  $\pm$  SEM of three independent experiments

**Figure S5. Effects of Mdivi-1, CCCP and DFP on mitophagy. Related to Figure 5.** HepG2 cells were treated with DMSO, Mdivi-1, CCCP or DFP for 24 hours. (A) Cells were lysed for the preparation of total cell lysates or for the isolation of mitochondria for immunoblot analysis. (B) Mitochondrial DNA (mtDNA) was quantified by qPCR and normalized against GAPDH DNA. The mtDNA level of control cells was arbitrarily defined as 1. The results represent the mean of at least three different experiments. (C) Analysis of mitophagy using the mKeima-Red reporter. Red color indicated mitophagy. Scale bar, 10  $\mu$ m. (D) Immunoblot analysis of cells without (Ctrl) and with treatment with DFP.

**Figure S6. PINK1 and the phosphorylation of S392 of p53. Related to Figure 6.** (A) HepG2 cells without treatment or with transfection of a control vector or the PINK1-expressing plasmid were lysed 48 hours after transfection and analyzed by immunoblot for phosphorylated ubiquitin, total ubiquitin, phosphorylated PARKIN, total PARKIN and PINK1. Actin served as the loading control. (B) Analysis of the effect of silencing of various kinases on the phosphorylation of S392 of p53. HepG2 cells transfected with various siRNAs for two days were lysed for immunoblot analysis. (C) Huh7 cells, which expressed p53(Y220C), were treated with the control siRNA (si-Ctrl) or si-PINK1 and lysed for immunoblot analysis. (D) Stable HepG2 cells that expressed the control shRNA (sh-Ctrl) or PINK1 shRNA (sh-PINK1) were lysed for immunoblot analysis. (E) Stable HepG2 cells with PINK1 knockdown were transfected with a control vector or a plasmid that expressed the shRNA-resistant wild-type PINK1 (left panel), or with a control vector or a plasmid that expressed the PINK1-kinase dead mutant (PINK1mt) (right panel) followed by immunoblot analysis.

**Figure S7. Role of PINK1 in p53 phosphorylation and tumorigenesis. Related to Figure 6.** (A) GST-PARKIN was mixed with GST-PINK1 or GST and incubated in the presence of ATP. The phosphorylation of PARKIN at S65 was then analyzed with the antibody that recognized phosphorylated S65. GST-PARKIN, GST-PINK1 and GST used for the reaction was also analyzed by anti-PARKIN, anti-PINK1 and anti-GST antibodies, respectively (bottom three panels). (B) The phosphorylation of ubiquitin by GST-PINK1 was conducted the same way as in (A), with the exception that GST-PARKIN was replaced with tetraubiquitin. (C) The

phosphorylation analysis of GST-p53 was conducted the same way as described in the legend to Figure 6E, with the exception that  $\gamma$ -<sup>32</sup>P-ATP was used for the labeling reaction and the phosphorylated protein was analyzed by autoradiography. (D) The representative SiMPull images are shown on the top. The chart demonstrated a dose-dependent binding of GST-p53 by PINK1. The K<sub>d</sub> was estimated to be ~5 nM. (E) HepG2 cells without or with treatment of DMSO or 3-MA as well as stable HepG2 cells that expressed sh-Ctrl, sh-ATG5 or sh-ATG7 were lysed for immunoblot analysis. (F) Stable HepG2 cells that expressed sh-Ctrl, sh-Atg5 or sh-Atg5 and sh-PINK1 were lysed for immunoblot analysis. (G) CD133<sup>+</sup> cells of the cell lines shown in (F) were subcutaneously injected into nude mice for tumorigenesis studies. Tumor imaging was conducted 3 months later. Representative tumor images were shown to the left and the quantification of photons, which reflected tumor sizes, were shown in the chart to the right.

**Figure S1**

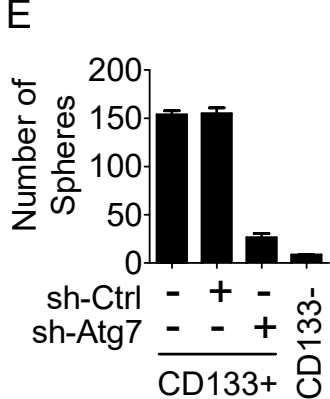
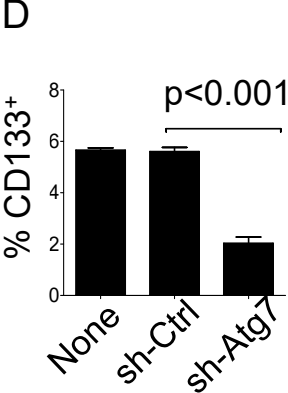
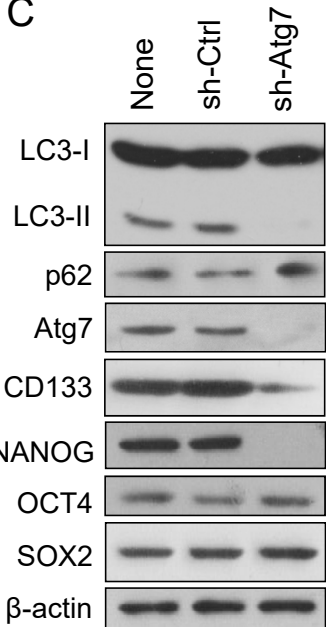
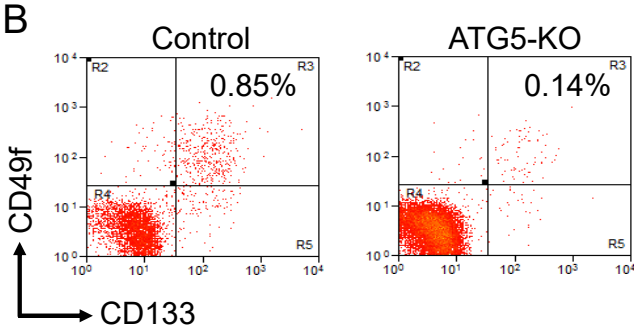
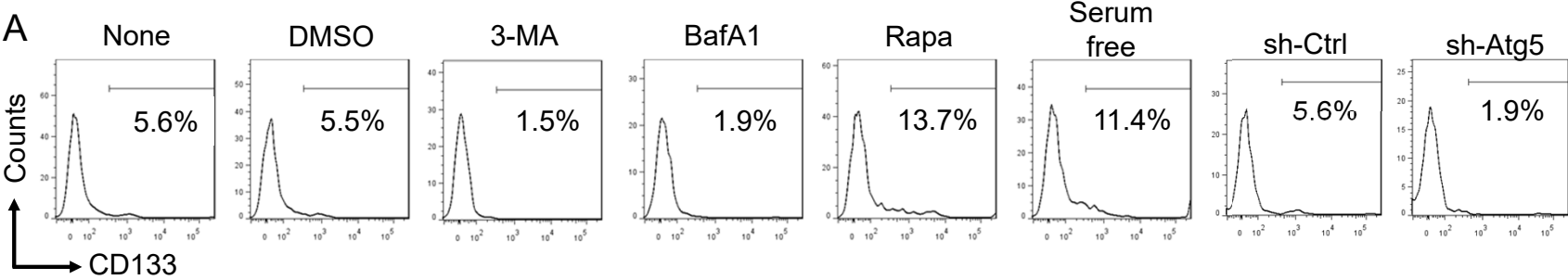


**Figure S2**

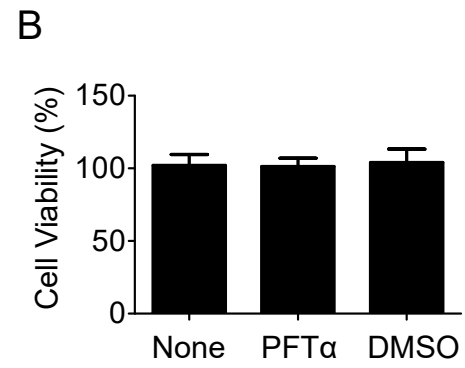
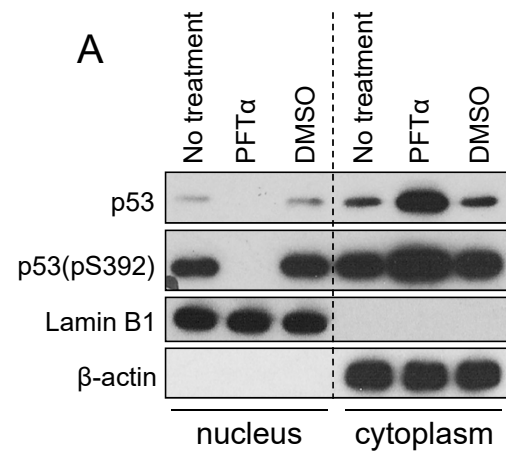


**Figure S3**

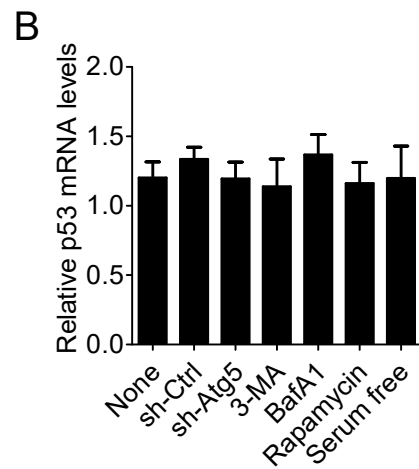
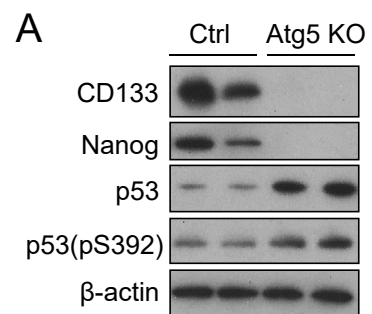




**Figure S5**

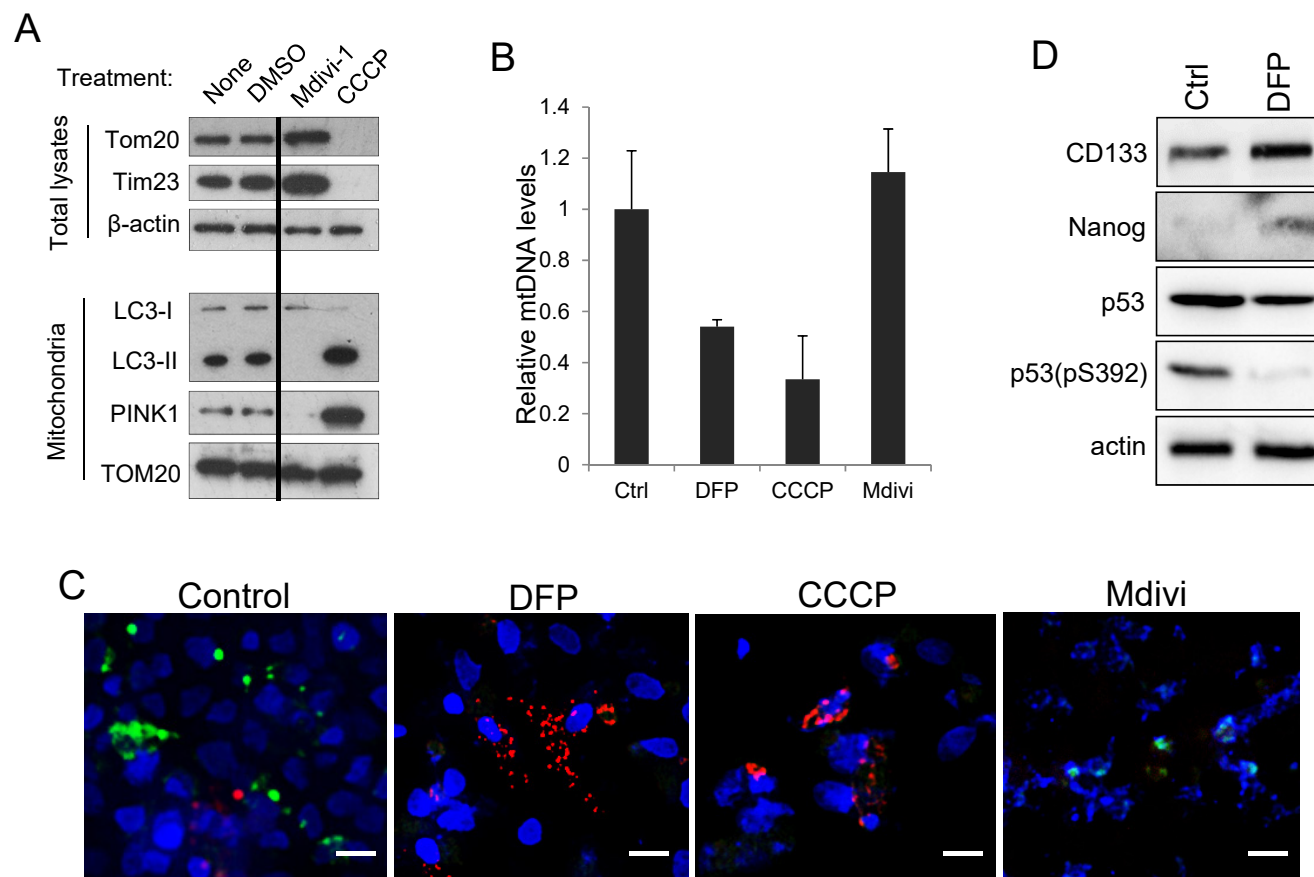




**Figure S6**

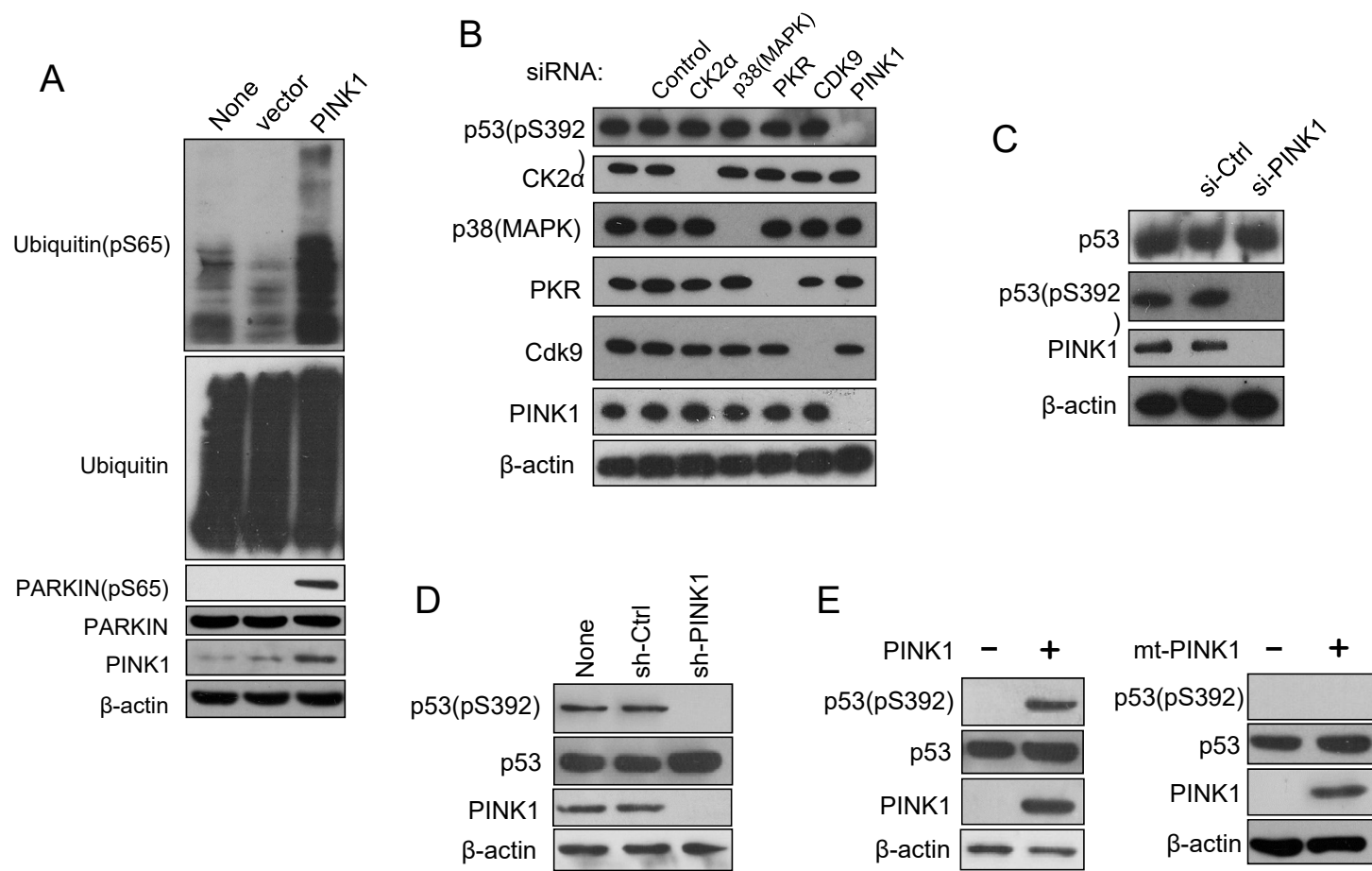


**Figure S7**

